Non-specular scattering from multilayer mirrors at normal incidence

E. M. Gullikson[a], D. G. Stearns[b], D. P. Gaines[b] and J. H. Underwood[a]

[a]Center for X-Ray Optics
Lawrence Berkeley National Laboratory
Berkeley, California 94720 USA

[b] Advanced Microtechnology Program
Lawrence Livermore National Laboratory
Livermore, California 94550 USA

ABSTRACT

The first measurements are reported of non-specular scattering of EUV radiation normally incident on a multilayer mirror. The scattering from a Mo/Si multilayer mirror has been measured as a function of angle and wavelength. A peak in the angular distribution of scattered light is observed which is due to the correlation of the roughness of different interfaces. The scattering from correlated roughness can be described by a simple kinematic theory of scattering. In the region of the Bragg reflectivity peak dynamical effects lead to a reduction in the scattering from the simple kinematic theory. The total integrated scatter (TIS) has been measured and is found to peak on the short wavelength side of the Bragg peak. The TIS is less than 1% of the incident intensity.

Keywords: non-specular scattering, multilayers, EUV lithography, roughness

1. INTRODUCTION

Normal incidence optics in the extreme ultraviolet (EUV) are central[1] to EUV lithography, astronomy, and microscopy. Multilayer coatings of Mo/Si and Mo/Be have been fabricated with reflectivities approaching 70% at normal incidence for wavelengths in the range of 11 to 14 nm. In general the measured reflectivity is lower than the theoretical. It is not known to what extent the observed loss in reflectance is due to interfacial roughness as opposed to interlayer diffusion. Interfacial roughness is distinguishable from interdiffusion in that it will produce non-specular scattering. If the shortfall of the reflectivity were to end up as scattered light within the field of view of an imaging system, the image contrast would be seriously degraded.

There has been substantial progress made in the past 10 years on the understanding of roughness in multilayers. Much of the knowledge comes from x-ray scattering experiments at grazing incidence beginning with those of Savage *et. al.*[2] and Kortright[3] and more recently by Salditt *et. al.*[4] There has also been much progress made in the scattering theory. The simple kinematic theory has been described by Sinha[5] and we outline those results in Section 2. The dynamical effects of the incident field have been included in the "specular field approximation" by Stearns.[6,7] The dynamical effects in both the incident and scattered field are described in the distorted-wave Born approximation (DWBA) developed by Holy and co-workers.[8,9]

There has been only one attempt[10] at measuring the non-specular scatter at normal incidence in the soft x-ray region and none was observed. The measurements in reference 10 were limited to 10^{-5} of the incident intensity. Because of the high brightness available at the Calibrations and Standards beamline 6.3.2 at the Advanced Light Source,[11] we were able to measure down to between $10^{-9} - 10^{-10}$ of the incident intensity which was more than sufficient to observe the scattering. The incident beam profile is shown in figure 1 along with the measured scattering distribution for a Mo/Si multilayer at normal incidence.

Proceedings of the SPIE Vol. 3113-55 (July 1997)
Please send correspondence to EMGullikson@lbl.gov.
D. G. Stearns is presently an independent consultant, email:healthst@ricochet.net.
D. P. Gaines is presently at Ultratech Stepper.

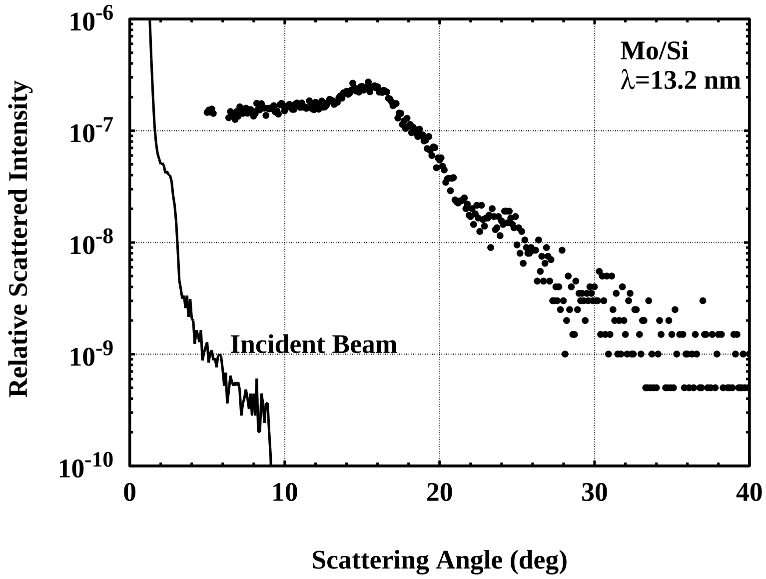

Figure 1. Measurements of non-specular scattering at normal incidence for a Mo/Si multilayer mirror. The incident wavelength, 13.2 nm, was just below the Bragg peak at 13.4 nm. At small angles the tail of the incident beam is also shown. The dynamic range is approaching 10 orders of magnitude.

2. THEORY

Correlation of the roughness plays a central role in determining the scattering from a multilayer. The importance of interlayer correlation was demonstrated very clearly in the experimental work of Savage *et. al.*[2] and Kortright.[3] If the roughness is correlated from layer to layer then the scattering from each interface adds coherently resulting in an interference structure in the scattered light. The scattered light adds in phase when

$$\mathrm{m}\lambda = d(\sin\theta_1 + \sin\theta_2). \tag{1}$$

Where θ_1 is the angle of incidence and θ_2 is the scattering angle, both measured with respect to the scattering surface. Although this equation is very similar to the grating equation, it is more of a generalization of Bragg's law since d is the multilayer period. Equation (1) is simply expressed in terms of the scattering vector

$$q_z = 2\pi/d \quad \text{where} \quad \mathbf{q} = \mathbf{k}_2 - \mathbf{k}_1. \tag{2}$$

$\mathbf{k}_1$ and $\mathbf{k}_2$ are the incident and scattered wave vectors, respectively and $|k_1| = |k_2| = 2\pi/\lambda$. This phenomenon is sometimes referred to as "quasi-Bragg scattering" or "resonant diffuse scattering". At high spatial frequencies the roughness becomes uncorrelated. The transition from correlated to uncorrelated roughness has been observed by Salditt *et. al.*[4] In the following section, the scattering distribution is calculated in the Born approximation.

2.1. Born approximation for a single rough surface

The simplest quantitative theory of scattering is given by the Born approximation. Although, as mentioned above, there are more accurate descriptions which account for the dynamical effects within the multilayer, these can be rather complicated and it is easy to lose track of the basic physics. In the following we outline the theory, for a more complete discussion see the work of Sinha *et. al.*[5,12] The differential cross section for x-rays scattered by a system is given in the Born approximation by

$$\frac{\mathrm{d}\sigma}{\mathrm{d}\Omega} = \left| \int_V n r_e f e^{-i\mathbf{q}\cdot\mathbf{r}} dV \right|^2 \tag{3}$$

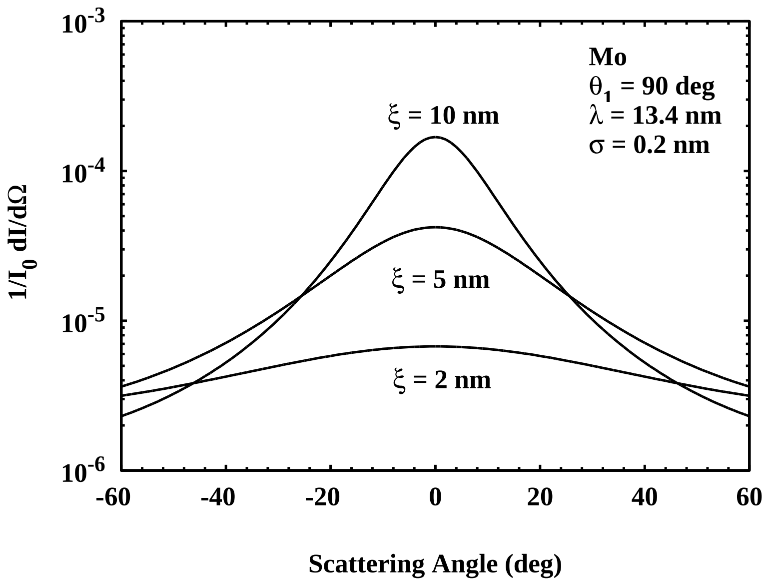

Figure 2. The scattering from a single rough surface of Mo calculated in the Born approximation for three values of the correlation length ξ. As the correlation length becomes longer the scattering is concentrated at smaller angles.

for s-polarized radiation, where n is the atomic density, f is the atomic scattering factor and $r_e = e^2/mc^2$ is the classical electron radius. These are simply related to the dielectric constant of the material by $nr_ef = k^2(1-\epsilon)/(4\pi)$ where $k = 2\pi/\lambda$. It can be shown[12] that for a rough surface where the surface height, $z(x,y)$, is a Gaussian random variable

$$\frac{\mathrm{d}\sigma}{\mathrm{d}\Omega} = n^2 r_e^2 \left|f\right|^2 AS(\mathbf{q}), \tag{4}$$

where A is the illuminated area of the surface and $S(\mathbf{q})$ is the scattering function given by

$$S(\mathbf{q}) = \frac{1}{q_z^2} \int\int_S dxdy e^{-q_z^2 g(x,y)/2} e^{-i(q_x x + q_y y)}. \tag{5}$$

The function $g(x,y) = \langle [z(0,0) - z(x,y)]^2 \rangle$ contains the statistical description of the roughness. For most surfaces of interest $g(x,y)$ reaches a finite value at large x, y and

$$g(x,y) = 2\left(\sigma^2 - C(x,y)\right) \tag{6}$$

where $C(x,y) = \langle z(0,0) z(x,y) \rangle$ is the correlation function. In this case we can separate the specular and diffuse scattering

$$S(\mathbf{q}) = S_{\text{specular}}(\mathbf{q}) + S_{\text{diffuse}}(\mathbf{q}). \tag{7}$$

If the amplitude of the roughness is sufficiently small ($q_z \sigma << 1$) then we obtain the simple result

$$S_{\text{diffuse}}(\mathbf{q}) = e^{-q_z^2\sigma^2} \int\int_S dxdy C(x,y) e^{-i(q_x x + q_y y)} \approx \text{PSD} \tag{8}$$

and the scattering function is simply related to the *power spectral density* (PSD) of the surface roughness.

The differential scattering cross section is defined in terms of the incident flux F_0 and the scattered flux F_s at a distance R by

$$\frac{\mathrm{d}\sigma}{\mathrm{d}\Omega} = \frac{R^2 F_s}{F_0}. \tag{9}$$

However in the laboratory one usually measures intensities. The quantity most readily compared with measurements is the fraction of the incident intensity which is scattered into a differential solid angle. This is related to the differential scattering cross section by

$$\frac{1}{I_0}\frac{\mathrm{d}I}{\mathrm{d}\Omega} = \frac{R^2 F_s}{F_0 A_0} = \frac{1}{A_0}\frac{\mathrm{d}\sigma}{\mathrm{d}\Omega}. \tag{10}$$

For the experimental geometry used here the cross-sectional area of the incident beam, $A_0 = A\sin\theta_1$, is constant. In this case both the differential scattering cross-section and $1/I_0(\mathrm{d}I/\mathrm{d}\Omega)$ vary as $1/\sin\theta_1$ due to the change in the illuminated surface area with incidence angle, θ_1.

The scattering distribution is then given by

$$\frac{1}{I_0}\frac{\mathrm{d}I}{\mathrm{d}\Omega} = \frac{k^4|1-\epsilon|^2}{16\pi^2\sin\theta_1}S(\mathbf{q}) = \frac{q_z^4}{16\pi^2\sin\theta_1}R(q_z)S(\mathbf{q}) \tag{11}$$

where $R(q_z) = |1-\epsilon|^2(k/q_z)^4$ is the Fresnel reflectivity when the angle of incidence is greater than the critical angle. For angles near and below the critical angle where the reflectivity can approach unity, the Born approximation is not expected to work. In this case the scattering must be calculated using the distorted-wave Born approximation[12] (DWBA) or the results of the vector scattering theory.[1,13]

To proceed we must make some assumption about the PSD of the surface. If we assume a simple exponential form for the correlation function, i.e.

$$C(R) = \sigma^2 e^{-R/\xi}, \tag{12}$$

then the PSD is given by

$$\mathrm{PSD} = \frac{2\pi\sigma^2\xi^2}{(1+q_r^2\xi^2)^{3/2}} \tag{13}$$

where $q_r^2 = q_x^2 + q_y^2$ and ξ is the in-plane radial correlation length. This form of the PSD reflects *conventional finish* and may not be representative of a polished surface which often exhibits fractal behavior.[14] However it appears to be a reasonable assumption if the roughness results from the growth of a film on a smooth substrate.[15] Figure 2 shows the scattering at normal incidence from a single surface of Mo using the PSD given in equation (13) for various values of the correlation length ξ. As the correlation length increases, the PSD is weighted toward larger scale roughness and the scattering is concentrated at angles closer to specular direction.

2.2. Kinematical theory for scattering from a multilayer

The scattering theory above may be generalized to the case of multiple interfaces. The scattering distribution is then

$$\frac{1}{I_0}\frac{\mathrm{d}I}{\mathrm{d}\Omega} = \frac{k^4}{16\pi^2\sin\theta_1}\sum_{i,j}\Delta\epsilon_i\Delta\epsilon_j^* e^{-iq_z(z_i-z_j)}S_{ij}(\mathbf{q}), \tag{14}$$

where $\Delta\epsilon_i$ is the change in dielectric function across the i-th interface and the scattering function is

$$S_{ij}(\mathbf{q}) = \frac{e^{-q_z^2(\sigma_i^2+\sigma_j^2)/2}}{q_z^2}\int\int_S dx\,dy(e^{q_z^2 C_{ij}(x,y)}-1)e^{-i(q_x x+q_y y)}. \tag{15}$$

$C_{ij}(\mathbf{R}) = \langle\delta z_i(0)\delta z_j(R)\rangle$ is the generalized correlation function which describes the correlation of the i-th and j-th interfaces.

In the limit that the roughness is perfectly conformal then $C_{ij}(\mathbf{R}) = C(\mathbf{R})$ for all i,j. The diffuse scattering distribution is then given by the particularly simple result

$$\frac{1}{I_0}\frac{\mathrm{d}I}{\mathrm{d}\Omega} = \frac{q_z^4}{16\pi^2\sin\theta_1}R(q_z)S(\mathbf{q}) \quad \text{where} \quad R(q_z) = \left|\frac{k^2}{q_z^2}\sum_i \Delta\epsilon_i e^{-iq_z z_i}\right|^2. \tag{16}$$

This expression for the scattering is identical to equation (11) which describes the scattering from a single surface, except here $R(q_z)$ is the multilayer reflectivity calculated in the kinematic approximation. Since the multilayer reflectivity has a maximum at the Bragg condition, the scattering is concentrated in the plane given by $q_z = 2\pi/d$. Thus, equation (16) describes the phenomenon of resonant diffuse scattering. Multiple reflections have been ignored for both the incident and scattered beams. These multiple reflections are clearly important in the vicinity of the Bragg peak where the reflectivity for Mo/Si can approach 67%. When either the incident or scattered wave is near the Bragg condition a dynamical theory of scattering is required.

3. EXPERIMENT

The Mo/Si multilayers used in these experiments were deposited by magnetron sputtering at LLNL on 1 inch diameter superpolished flats (General Optics Inc., Moorpark, CA). The PSD of the substrate was measured using an atomic force microscope and was approximately given by PSD(Å^4) $= 25/f^{0.9}$ where f is the spatial frequency in units of Å^{-1}. The multilayer was deposited with 40 periods, a d-spacing of 6.87 nm and a ratio of the Mo thickness to d-spacing of $\Gamma = 0.37$. The experiments were performed at the Advanced Light Source on the Calibrations and Standards beamline 6.3.2. The beamline uses the radiation from a bending magnet and was designed for making absolute measurements in the 50 eV to 1000 eV energy range.[11] The monochromator uses a variable line spaced plane grating to achieve high spectral resolution. The typical spectral resolution for these measurements was approximately 1 part in 2000 but can be as high as 1 part in 7000. The combination of a Si filter and a triple bounce order suppressor was used to eliminate the higher order light from the monochromator. As a result the light reaching the sample had a purity estimated to be better than 99.9%.

A set of apertures were installed in the beamline just upstream of the reflectometer endstation. These were necessary in order to block the radiation scattered from the beamline optics. The profile of the incident beam is shown in figure 1. All of the measurements were performed with s-polarized radiation. That is the electric field of the incident light was in a horizontal plane and the scattering was measured in a vertical plane.

A channel electron multiplier (CEM) was used for the scattering measurements. In order to put the scattering on an absolute scale the incident intensity was measured with a GaAsP photodiode and the efficiency of the CEM was measured relative to the photodiode using an intensity where both detectors could be used. The detection efficiency of the CEM was approximately 5% for the wavelength range of interest.

For most of the measurements, a 2 mm diameter circular aperture was used in front of the detectors to limit the angular resolution. Since the detectors were positioned 225 mm away from the sample, the angular resolution was 0.5 degrees and the solid angle collected was 6.2e-5 steradian. (The initial data shown in figure 1 were taken with a smaller detector aperture.)

The total integrated scatter (TIS) was measured using an annular Si photodiode (AXUV-PS2 from International Radiation Detectors, Torrance, CA). The efficiency of the Si photodiode is well known and was cross calibrated with the GaAsP photodiode. The active area of the diode is 10mm x 10mm with a central hole 1mm x 2mm. The detector was positioned 5 mm away from the sample surface so that it accepted scattered radiation between about 8 deg and 45 deg from the normal.

4. RESULTS

The angular distribution of scattering is shown in figure 3. The scattering angle is measured from the specular beam, i.e. the surface normal. At the Bragg peak, 13.4 nm, the scattered light is peaked at the multilayer normal, scattering angle = 0. As the wavelength is reduced the distribution peak moves away from the normal. This is characteristic of resonant diffuse scattering described by equation (1). Assuming that the scattering is symmetric around the incident beam, the scattered light is concentrated in a ring which grows in diameter as the wavelength is reduced. The dashed curves were calculated using equation (16) and assuming the simple form of the PSD given in equation (13). The kinematic model works quite well for the shorter wavelengths 12.6, 12.8 nm. However, in the region where either the incident or the scattered wave is close to satisfying the Bragg condition, multiple reflections lead to extinction and the scattering is reduced from what is calculated with the kinematic model. This is clear in the distribution for 13.0 nm where the extinction of the scattered light produces the sharp peak at about 19 deg. The region of the Bragg peak is of course the most interesting from a practical perspective since this is where the multilayer would be used in an imaging system. In order to describe the scattering at the Bragg peak a dynamical

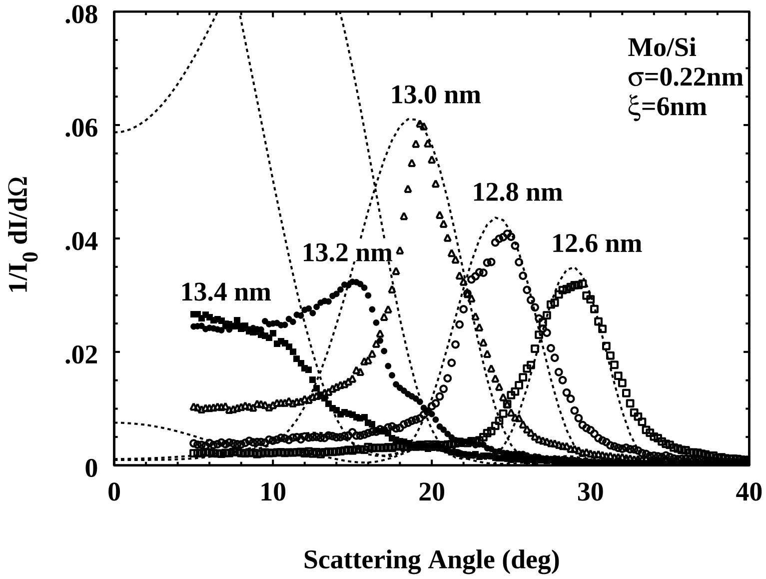

Figure 3. Non-specular scattering angular distribution for EUV light at normal incidence on a Mo/Si multilayer mirror. At the peak of the reflectance curve, 13.4 nm, the scattering is maximum is at 0 degrees, measured from the normal. The peak of the scattering moves away from the normal as the wavelength is reduced. This is characteristic of vertically correlated roughness. The dashed lines are fit using the Born approximation described in the text.

model for scattering is required, such as formulated by Stearns[7] or the DWBA.[8,9] This work is in progress and will be the topic of a future publication.

The measurements shown in figure 3 demonstrate the high degree of vertical correlation of the roughness in the multilayer stack. For short enough length scales the roughness must become uncorrelated.[4] It is clear from the measurements presented in figure 3 that the roughness is correlated for scattering angles as large as 30 deg, which corresponds to in-plane length scales of $2\lambda = 26$ nm.

If the measured PSD of the substrate is used in (16) to calculate the non-specular scattering, the results are approximately 6 to 8 times smaller than those shown in figure 3 (for 12.6-13.0 nm). Thus, although the roughness that is responsible for the observed scattering is highly correlated it is not simply replicated substrate roughness. Rather it is roughness which develops within the multilayer coating itself. It is expected then that the PSD of each interface should actually increase from the bottom to the top of the stack.[15] Thus the PSD which results from the fits of figure 3 may be interpreted as an effective PSD for the multilayer, which will correspond to some sort of average over the PSDs of the individual interfaces. A more complete model should include the variation in the PSD through the multilayer.

In figure 4, the total integrated scatter (TIS) is shown versus wavelength. As a result of the vertical correlation that leads to the resonant diffuse scattering shown in figure 3, the TIS is peaked on the short wavelength side of the reflectivity maximum. For wavelengths longer than the Bragg peak, 13.4 nm, it is impossible to satisfy equation (1) for any scattering angle and the TIS is low. For shorter wavelengths, equation (1) is satisfied at some angle and the scattered light adds in phase to produce the resonant diffuse scattering peak shown in figure 3. Close to the Bragg peak at 13.4 nm, much of the scattered light goes back through the central hole in the photodiode. Thus the scattering here is underestimated. At 13.4 nm it is estimated that only about one half of the scattered light is being collected. This was verified by increasing the distance of the photodiode to the sample. The TIS is less than 1% at the Bragg peak for this multilayer. This is to be compared with the 7% shortfall of the measured reflectance from the theoretical maximum performance. Thus, most of the observed reduction in reflectance is due either to interdiffusion or very high frequency roughness.

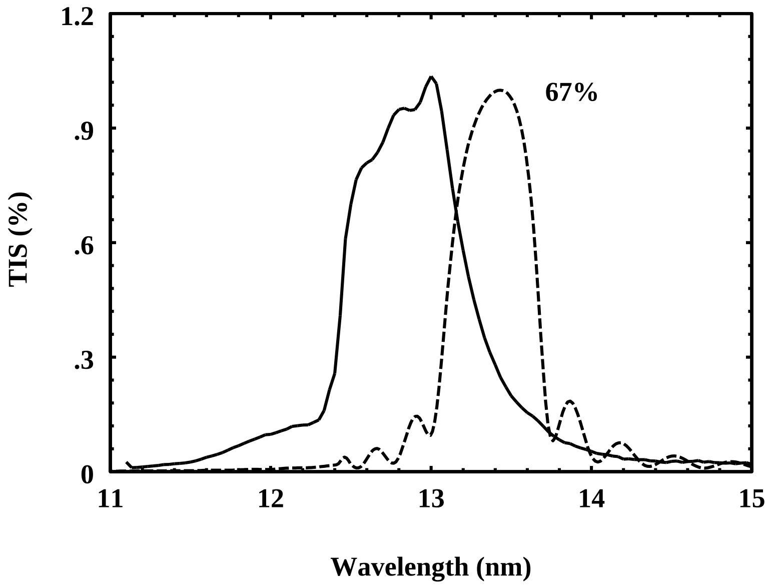

Figure 4. Measurement of the total integrated scatter (TIS, solid curve) from a Mo/Si multilayer at normal incidence. The normal incidence reflectivity (dashed curve) is scaled down to fit on the same plot. The TIS is *blue-shifted* from the multilayer reflectivity and drops sharply at the Si $L_{2,3}$ edge (12.4 nm).

It is interesting to note that the amount of scattered light collected during a typical measurement of the specular reflectance is negligible. For example, we normally use a photodiode 4.6mm x 4.6mm at a distance of 225 mm from the sample ($\theta = 20$ mrad). For the Mo/Si multilayer used here the contribution of scattered light to the measured reflectance would be $1/I_0(dI/d\Omega) \times \pi\theta^2/4 = 10^{-5}$.

5. CONCLUSIONS

The angular distribution of scattering exhibits a peak indicative of vertically correlated roughness which can be described by a simple kinematic theory in regions away from the Bragg condition for either the incident or scattered waves. The non-specular scattering apparently results from roughness which develops in the multilayer coating as opposed to substrate roughness. This roughness is highly correlated for in-plane periods as short as 26nm. A more complete description can be obtained by including the dynamic or standing wave effects and will be reported in a future publication. The total integrated scatter has been measured and found to be *blue-shifted* from the Bragg maximum. The total integrated scatter in a high quality Mo/Si multilayer is less than 1%.

ACKNOWLEDGEMENTS

We wish to thank Claude Montcalm for many useful conversations. This work was supported by Intel and the Office of Basic Energy Sciences, U. S. Department of Energy. Construction of the beamline was funded by the Advanced Lithography Program of the Advanced Research Projects Agency (ARPA).

REFERENCES

1. E. Spiller, *X-ray Optics*, SPIE, Bellingham, WA, 1994.
2. D. E. Savage, J. Kleiner, N. Schimke, Y.-H. Phang, T. Jankowski, J. Jacobs, R. Kariotis, and M. G. Lagally, "Determination of roughness correlations in multilayer films for x-ray mirrors," *J. Appl. Phys.* **69**, pp. 1411–1424, 1991.
3. J. B. Kortright, "Non-specular scattering from multilayer structures," *J. Appl. Phys.* **70**, p. 3620, 1991.

4. T. Salditt, D. Lott, T. H. Metzger, J. Peisl, G. Vignaud, P. Hoghoj, O. Scharpf, P. Hinze, and R. Lauer, "Interfacial roughness and related growth mechanisms in sputtered W/Si multilayers," *Phys. Rev. B* **54**, pp. 5860–5872, 1996.
5. S. K. Sinha, "X-ray diffuse scattering as a probe for thin film and interface structure," *J. Phys. III France* **4**, pp. 1543–1557, 1994.
6. D. G. Stearns, "The scattering of x-rays from nonideal multilayer structures," *J. Appl. Phys.* **65**, pp. 491–506, 1989.
7. D. G. Stearns, "X-ray scattering from interfacial roughness in multilayer structures," *J. Appl. Phys.* **71**, pp. 4286–4298, 1992.
8. V. Holy, J. Kubena, I. Ohlidal, K. Lischka, and W. Plotz, "X-ray reflection from rough layered systems," *Phys. Rev. B* **47**, pp. 15896–15903, 1993.
9. V. Holy and T. Baumbach, "Nonspecular x-ray reflection from rough multilayers," *Phys. Rev. B* **49**, pp. 10668–10676, 1994.
10. E. Spiller, D. G. Stearns, and M. Krumrey, "Multilayer x-ray mirrors: interfacial roughness, scattering and image quality," *J. Appl. Phys.* **74**, pp. 107–118, 1993.
11. J. H. Underwood, E. M. Gullikson, M. Koike, P. J. Batson, P. E. Denham, K. D. Franck, R. E. Tackaberry, and W. F. Steele, "Calibration and Standards beamline 6.3.2 at the Advanced Light Source," *Rev. Sci. Instrum.* **67**, 1996.
12. S. K. Sinha, E. B. Sirota, S. Garoff, and H. B. Stanley, "X-ray and neutron scattering from rough surfaces," *Phys. Rev. B* **38**, pp. 2297–2311, 1988.
13. E. L. Church, H. A. Jenkinson, and J. M. Zavada, "Relationship between surface scattering and microtopographic features," *Optical Engineering* **18**, pp. 125–136, 1979.
14. E. L. Church, "Fractal surface finish," *Applied Optics* **27**, pp. 1518–1526, 1988.
15. D. G. Stearns, "Stochastic model for thin film growth and erosion," *Appl. Phys. Lett.* **62**, pp. 1745–1747, 1993.